JACS
JOURNAL OF THE AMERICAN CHEMICAL SOCIETY

Article

pubs.acs.org/JACS

Ion Pair−π Interactions

Kaori Fujisawa, Marie Humbert-Droz, Romain Letrun, Eric Vauthey, Tomasz A. Wesolowski, Naomi Sakai, and Stefan Matile*

School of Chemistry and Biochemistry, University of Geneva, CH-1211 Geneva, Switzerland

Supporting Information

ABSTRACT: We report that anion−π and cation−π interactions can occur on the same aromatic surface. Interactions of this type are referred to as ion pair−π interactions. Their existence, nature, and significance are elaborated in the context of spectral tuning, ion binding in solution, and activation of cell-penetrating peptides. The origin of spectral tuning by ion pair−π interactions is unraveled with energy-minimized excited-state structures: The solvent- and pH-independent red shift of absorption and emission of push−pull fluorophores originates from antiparallel ion pair−π attraction to their polarized excited state. In contrast, the complementary parallel ion pair−π repulsion is spectroscopically irrelevant, in part because of charge neutralization by intriguing proton and electron transfers on excited push−pull surfaces. With time-resolved fluorescence measurements, very important differences between antiparallel and parallel ion pair−π interactions are identified and quantitatively dissected from interference by aggregation and ion pair dissociation. Contributions from hydrogen bonding, proton transfer, π−π interactions, chromophore twisting, ion pairing, and self-assembly are systematically addressed and eliminated by concise structural modifications. Ion-exchange studies in solution, activation of cell-penetrating peptides in vesicles, and computational analysis all imply that the situation in the ground state is complementary to spectral tuning in the excited state; i.e., parallel rather than antiparallel ion pair−π interactions are preferred, despite repulsion from the push−pull dipole. The overall quite complete picture of ion pair−π interactions provided by these remarkably coherent yet complex results is expected to attract attention throughout the multiple disciplines of chemistry involved.

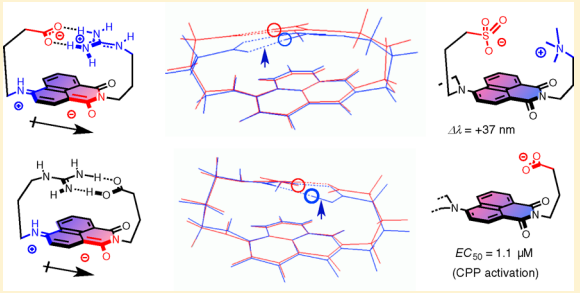

INTRODUCTION

In studies on anion−π interactions[1−4] and cation−π interactions,[5] counterions are often ignored. In this report, we ask whether both cation and anion could interact with the same aromatic surface. This question is of interest because cation−π interactions are by now very well known and appreciated,[5] and the complementary anion−π interactions, i.e., the binding of anions on π-acidic surfaces, are increasingly recognized[1] and used.[2−4] Contributions from counterions to these processes have received most attention in the context of cation−π interactions between guanidinium cations and π-basic aromatics.[6] This interest originates from the abundance of carboxylate−guanidinium−aromatic triads in peptides and proteins.[6] They are involved in molecular recognition processes in many variations. Importance in protein folding, long-distance charge transfer,[7] and cellular uptake[8] has been indicated as well. Particularly relevant in the context of this study are contributions to spectral tuning. The influence of nearby charges on the spectroscopic properties of chromophores is very well recognized. Nakanishi's external-point-charge model to rationalize the origin of color vision can serve as early example.[9] Today, the crystal structures are known and the charges are there indeed, including very interesting potential anion−π interactions, but it is also understood that the origin of color vision is much more complex.[10] Closer to the topic of this study are the clusters of ion pairs that tune the emission of fluorescent proteins.[11] However, only selected cations within these clusters localize on the polarized aromatic surfaces, whereas the anions are usually left on the side. The same is true for several elegant model systems with anions that are covalently positioned nearby to support the binding of cations on π-basic surfaces.[6] Explicit considerations of anions and cations bound on the same aromatic surface are extremely rare and either fully speculative[8] or explored on π surfaces that are small for this purpose.[12] Building on a preliminary communication on proof-of-principle by absorption spectroscopy and ground-state modeling,[13] the objective of this study was to explore ion pair−π interactions more comprehensively in the context of spectral tuning, ion binding in solution, and activation of cell-penetrating peptides (CPPs). Energy-minimized excited-state structures, time-resolved fluorescence measurements, and systematic structural modification to dissect and eliminate contributions from hydrogen bonding, proton transfer, π−π interactions, chromophore twisting, ion pairing, and aggregation are bundled to work out the existence, nature, and significance of ion pair−π interactions. Studies on coupled ion exchange in solution and the activation of CPPs reveal a preference for parallel ion pair−π interactions in the ground state that is complementary to the antiparallel ion pair−π

Received: May 30, 2015
Published: August 20, 2015

DOI: 10.1021/jacs.5b05593
J. Am. Chem. Soc. 2015, 137, 11047−11056

attraction in the excited state found to account for spectral tuning.

RESULTS AND DISCUSSION

Initial Results. Early on, we realized that the polarized surfaces of push–pull fluorophores[14,15] would be ideal to explore *ion pair–π interactions, i.e., cation–π and anion–π interactions that take place on the same surface.* The compact 4-amino-1,8-naphthalimides (ANIs)[15] were selected for this purpose (Figure 1).[13] Moreover, we realized that covalent

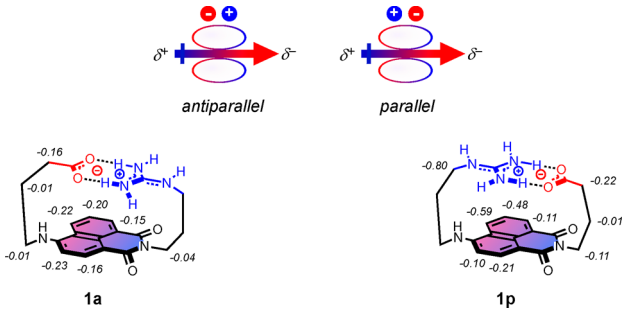

Figure 1. Definition of antiparallel and parallel ion pair–π interactions and their expression in the original covalent systems **1a** and **1p**, respectively. In the bottom images, shifts in the ^{1}H NMR spectral signals of **1a** and **1p** in DMSO-d_6 compared to their neutral precursors **1o** (see Figure 2) and the inverted counterpart are indicated in ppm.

approaches[4] would be needed to minimize ambiguities and control the positioning of the ion pair on the surface. Two complementary arrangements were defined. Ion pair–π interactions with anion–π interactions near the positive and cation–π interactions near the negative end of the push–pull dipole were designated as *antiparallel*. In the complementary *parallel* ion pair–π interactions, the ion pair and push–pull dipole are oriented in the same direction (Figure 1, top). The model system **1a** was designed to explore antiparallel ion pair–π interactions. A carboxylate anion was attached to the amine donor, and a guanidinium cation was attached to the imide acceptor. The length of the spacer was adjusted to support ion pairing on the push–pull surface with precisely sculpted Leonard turns, i.e., trimethylene chains folded in a half-chair conformation.[16]

In system **1p**, the same molecular handshake was arranged for parallel ion pair–π interactions. Initial results showed that the absorption maximum of **1a** was red-shifted by up to +41 nm against **1o** in the least polar solvent CCl_4. Decreasing red shifts for **1a** with increasing solvent polarity, aggregation, and carboxylate protonation and excellent agreement with computational simulations supported that antiparallel ion pair–π interactions account for the observed spectral tuning. These initial results on spectral tuning from absorption spectroscopy and ground-state modeling have been used for proof-of-principle in a preliminary communication.[13] In the following, we report the decisive experiments needed to understand spectral tuning by ion pair–π interactions (energy-minimized exited-state structures, time-resolved fluorescence, full structural analysis by synthetic modifications, etc.), together with studies on ion exchange in solution and the activation of CPPs.

Carboxylate–Guanidinium Pairs. The alkylated versions **2a** and **2p** were prepared to explore possible contributions from self-assembly and proton transfer in the excited state to spectral tuning (Figure 2). The attachment of the hexyl chain at the

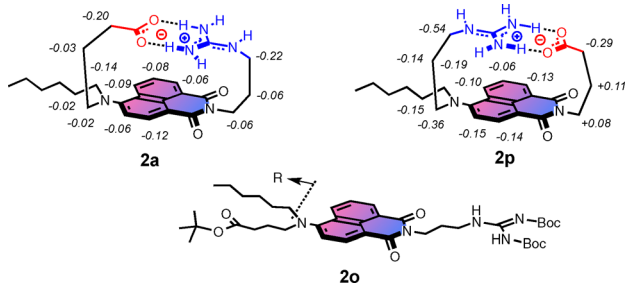

Figure 2. Covalent systems **2a** and **2p** for antiparallel and parallel ion pair–π interactions with alkylated amine donors to explore contributions from excited-state proton transfer, self-assembly, and fluorophore twisting. ^{1}H NMR shifts in DMSO-d_6 against their neutral precursors **2o** and the inverted counterpart **2i** are indicated in ppm (**1o**: R = H).

amine donor replaces the proton that could potentially cause problems in **1a** and **1p**. Already sufficiently acidic for sensing applications in the ground state,[15] intramolecular charge transfer in the excited state further increases the acidity of this proton. The resulting possibility of deprotonation and intramolecular proton transfer toward the anionic imide acceptor could result in spectroscopic changes that are unrelated to ion pair–π interactions. The long hexyl chain should also improve solubility in less polar solvents and thus minimize eventual contributions from dimeric sandwich structures of the facial amphiphiles, or from higher aggregates.

The alkylated ion pair–π system **2p** was prepared from the brominated naphthalanhydride **2b** (Scheme 1). Reaction with

Scheme 1. Synthesis of Ion Pair–π System 2p[a]

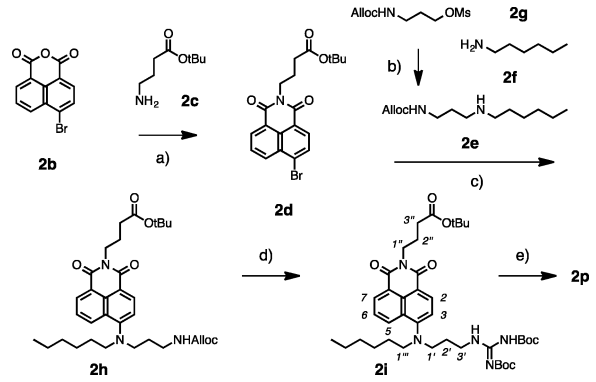

[a]Reagents and conditions: (a) TEA, DMF, 100 °C, μW, 2 h, 93%; (b) NaI, DMSO, 56%; (c) DMSO, 140 °C, 3 d, 10%; (d) 1. *p*-nitrophenol, Bu_3SnH, $Pd(PPh_3)_2Cl_2$, CH_2Cl_2, rt, 2 h; 2. *N,N′*-bis(*tert*-butoxycarbonyl)-1*H*-pyrazole-1-carboxamidine, TEA, DMF, rt, 2 h, 17% (two steps); (e) TFA, CH_2Cl_2, rt, 3 h, quant.

4-aminobutanoate **2c** gave imide **2d**. The secondary amine **2e** was readily accessible by alkylation of primary amine **2f** with the mesylate **2g**. Amination of bromonaphthalene **2d** with amine **2e** gave the final push–pull scaffold in **2h**. Removal of the Alloc protecting group followed by guanidinylation yielded the protected target molecule **2i**. Liberation of both charges under mild acidic conditions gave the parallel ion pair–π system **2p**. The antiparallel homologue **2a** was prepared correspondingly (Scheme S1 in the Supporting Information).

Comparison of the ^{1}H NMR spectra of **2p** and **2a** with ion-pair-free precursors revealed clear upfield shifts for all

DOI: 10.1021/jacs.5b05593
J. Am. Chem. Soc. 2015, 137, 11047–11056

naphthalene protons (Figure 2 and Figures S6 and S7 in the Supporting Information). These shifts indicated that ion pair−π interactions induce changes in the distribution of electron density within the naphthalene core. With very few exceptions, the shifts in the ^{1}H NMR spectra of **2p** and **2a** were similar but smaller than with **1p** and **1a** (Figure 1). An increased twist of the nitrogen−naphthalene bond caused by the added alkyl chain could account for the overall smaller differences, perhaps hindering the formation of ion pair−π interactions and weakening conjugation and the push−pull system slightly.

Absorption and emission spectra of control **2o** without ion pair−π interactions showed the positive solvatochromism that is characteristic for chromophores that are more polar in the excited than in the ground state (Figure 3c, blue to red with

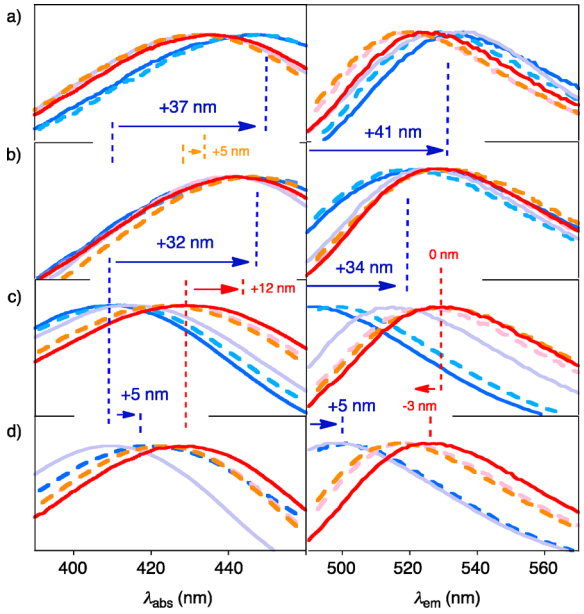

Figure 3. Absorption (left) and emission spectra (right) of **3a** (a), **2a** (b), and **2p** (d) compared to **2o** (c) in CCl_4 (blue), toluene (cyan), THF (purple), DMF (pink), DMSO (red), and MeCN (orange, compare Table 1). All spectra were normalized at their maximum.

increasing polarity). The maximal red shift in the absorption spectra from λ_{abs} = 410 nm in the least polar CCl_4 to λ_{abs} = 430 nm in the polar DMSO calculated to $\Delta\lambda_{abs}$ = +20 nm. In emission, a maximal red shift $\Delta\lambda_{em}$ = +39 nm from λ_{em} = 491 nm to λ_{em} = 530 nm was observed (Figure 3c, right). This positive solvatochromism of push−pull chromophores originates from the strong polarization of their first excited state by intramolecular charge transfer from the donor to the acceptor. In polar solvents, this polarized excited state is stabilized by dipole−dipole interactions with solvent molecules.[14,15] Compared to **1o** with λ_{abs} = 421 nm in CCl_4, the absorption maxima of **2o** was $\Delta\lambda_{abs}$ = −11 nm blue-shifted. Reduced chromophore polarization due to a slightly increased twist around the amine−naphthalene bond caused by the added alkyl group accounts for this less important bathochromic effect.

The absorption maximum of the alkylated ion pair−π system **2a** in the least polar solvent CCl_4 was at λ_{abs} = 442 nm (Figure 3b, left, blue; Table 1, entry 7). Compared to ion-pair-free controls, the antiparallel ion pair−π interactions in **2a** caused a red shift of $\Delta\lambda_{abs}$ = +32 nm (Figures 3b and 4; emission, $\Delta\lambda_{em}$ = +34 nm, Figure 3b; Table 1, entry 7). The red-shifted absorption of **2a** in nonpolar solvents suggested that antiparallel

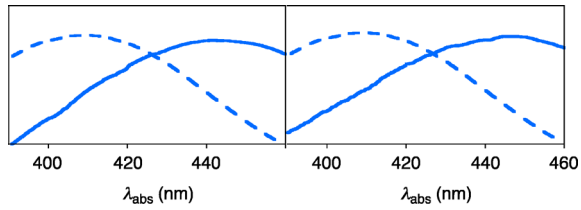

Figure 4. Absorption spectra of **2a** (solid, left), **3a** (solid, right), and **2o** (dashed) in CCl_4.

ion pair−π interactions stabilize the more polarized excited state **ES$_a$-A** much more than the less polarized ground state (Figure 5).

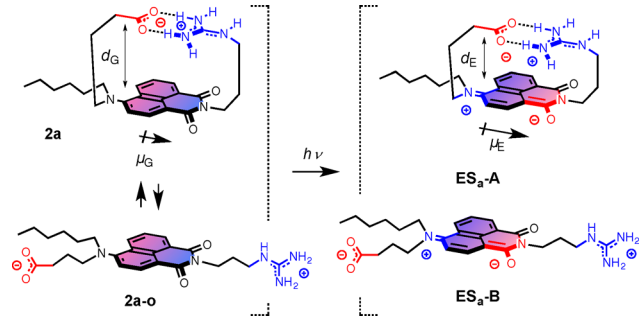

Figure 5. Structure of antiparallel ion pair−π system **2a**, open conformer **2a−o**, and their corresponding excited states **ES$_a$-A** and **ES$_a$-B**. Push−pull dipoles (μ) and distances between ion pair and π surface (d) in ground (G) and excited state (E) are indicated.

The red-shifted absorption maximum of **2a** was independent of the polarity of the solvent (Figure 3b, left, blue to red with increasing polarity). Compared to maximal λ_{abs} = 430 nm with **2o**, the absorption maxima up to λ_{abs} = 446 nm of **2a** remained strongly red-shifted even in the most polar solvent (Figure 3b vs c, left, red). This constant red shift suggested that antiparallel ion pair−π interactions in **2a** persist under more competitive conditions, and that the stabilization of the polarized excited state by ion pair−π interactions in **ES$_a$-A** significantly exceeds stabilization by polar solvents (Figure 5). Similarly weak solvatochromism found in emission spectra of **2a** (Figure 3b, right) confirmed the dominant role played by antiparallel ion pair−π interactions in spectral tuning. Eventual contributions from the open form **ES$_a$-B** in the excited state are thus minor (Figure 5).

Absorption and emission spectra of **2a** and **1a** followed overall quite similar trends (Table 1). This similarity implied that neither (i) deprotonation of the amine donor in the excited state, (ii) twisting of the amine donor out of conjugation by an additional alkyl substituent, nor (iii) fluorophore aggregation contributes significantly to the observed spectral tuning by antiparallel ion pair−π interactions.

The absorption and emission spectra of **2p** showed positive solvatochromism similar to control **2o** (Figure 3c vs d). This similarity indicated that the contributions from parallel ion pair−π interactions to spectral tuning are weak, nearly negligible. Neutralization of the parallel ion pair by intramolecular proton transfer could account for this finding. Results from computational studies supported the occurrence of proton transfer to remove increased ion pair−π repulsion on the polarized push−pull surface in the excited state (see below). However, charge neutralization by proton transfer was not

DOI: 10.1021/jacs.5b05593
J. Am. Chem. Soc. 2015, 137, 11047−11056

Table 1. Steady-State Spectroscopic Properties of Parallel and Antiparallel Ion Pair–π Interactions[a]

entry	solvent[b]	cpd[c]	λ_{abs} (nm)[d]	$\Delta\lambda_{abs}$ (nm)[e]	λ_{em} (nm)[f]	$\Delta\lambda_{em}$ (nm)[g]	cpd[c]	λ_{abs} (nm)[d]	$\Delta\lambda_{abs}$ (nm)[e]	λ_{em} (nm)[f]	$\Delta\lambda_{em}$ (nm)[g]
1	CCl_4[h]	**1a**[i]	462	+41	562	+68	**1p**[i]	449	+28	549	+55
2	toluene[j]										
3	THF		444	+14	518	+18		436	+6	501	+1
4	DMF		452	+12	528	+8		435	−5	524	+4
5	DMSO		457	+13	534	+10		440	−4	524	0
6	MeCN		447	+14	523	−8		438	+5	518	+3
7	CCl_4	**2a**	442	+32	525	+34	**2p**	–[j]			
8	toluene		444	+31	519	+21		418	+5	502	+5
9	THF		440	+25	526	+11		409	−6	499	−16
10	DMF		439	+13	530	+4		423	−3	520	−6
11	DMSO		442	+12	530	0		429	−1	527	−3
12	MeCN		446	+23	532	+3		424	+1	517	−12
13	CCl_4	**3a**	447	+37	532	+41	**2o**	410		491	
14	toluene		448	+35	529	+31		413		498	
15	THF		433	+18	532	+17		415		515	
16	DMF		434	+8	521	−5		426		526	
17	DMSO		435	+5	526	−4		430		530	
18	MeCN		433	+10	519	−10		423		529	

[a]Left side, antiparallel (**a**) compounds; right side, parallel (**p**) and open (**o**) compounds. For original data and conditions, see Figures 3 and 7. [b]Polarity E_T^N: CCl_4, 0.052; toluene, 0.099; THF, 0.207; DMF, 0.386; DMSO, 0.444; MeCN, 0.460. [c]For structures, see Figures 1, 2, and 6. [d]Wavelength of absorption maximum; excitation maxima showed nearly identical trends. [e]Shift of λ_{abs} compared to λ_{abs}^0 of ion-pair-free **1o** (for **1a**, **1p**) or **2o** (for **2a**, **2p**, **3a**). [f]Wavelength of emission maximum (excitation at λ_{abs}). [g]Shift of λ_{em} compared to λ_{em}^0 of ion-pair-free **1o** or **2o**. [h]Decreasing shifts with increasing concentration suggested that monomeric systems are measured at saturation with dilution.[13] [i]Some data for these two compounds are taken from ref 13. [j]Not measured because of poor solubility.

observed in computational analysis of the ground state of **2p** (below),[13] and comparison of the NMR shifts suggested that the ion pairs exist in both **2a** and **2p** (Figure 2). The poor influence of parallel ion pair–π interactions on the absorption spectra of **2p** thus requires most likely another explanation. Electron transfer around the transferable proton toward neutral guanidine and carboxyl radicals during excitation could be considered as reasonable possibility to minimize parallel ion pair–π repulsion in the Franck–Condon state. Dependence of the solvatochromism in absorption spectra on hydrogen bonding has been observed previously.[14]

Sulfonate–Tetraalkylammonium Pairs. In the covalent system **3a**, the carboxylate–guanidinium pairs are replaced by sulfonate–tetraalkylammonium pairs (Figure 6). These "pure"

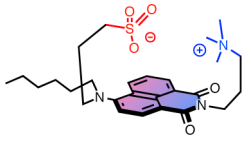

3a

Figure 6. Covalent system **3a** for antiparallel ion pair–π interactions with sulfonate–tetraalkylammonium pairs to explore contributions from π–π interactions and hydrogen bonding.

ion pairs lack planar π systems for supportive π–π interactions and acidic hydrogens for supportive hydrogen bonds. This antiparallel system **3a** was synthesized from the previously introduced anhydride **2b** (Scheme 2). Imide formation with the primary amine in diamine **3b** gave imide **3c**. The secondary amine **3d** was easily accessible from 1,3-propanesultone **3e** and hexylamine **2f**. Amination of the bromonaphthalene **3c** under quite harsh conditions gave sulfonate **3f**, and methylation of the

Scheme 2. Synthesis of Ion Pair–π System 3a[a]

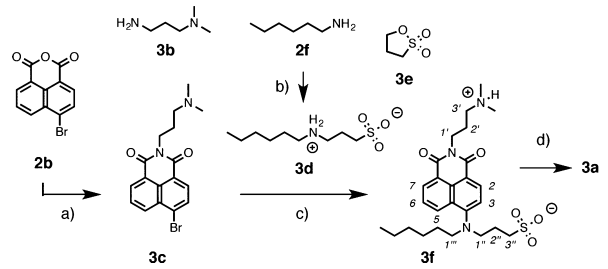

[a]Reagents and conditions: (a) TEA, DMF, 100 °C, μW, 2 h, 9%; (b) toluene, rt, 15 h, 40%; (c) DMSO, TEA, 120 °C, 3 d, 33%; (d) MeI, $CHCl_3$, 90 °C, 3 d, 18%.

tertiary amine with methyl iodide afforded the target molecule **3a**.

In nonpolar solvents, the absorption maximum of the "pure" ion pair–π system **3a** was at λ_{abs} = 447 nm (Figure 3a, left, blue; Table 1, entry 13). Compared to control **2o** without ion pair–π interactions, this calculated to a red shift $\Delta\lambda_{abs}$ = +37 nm that was even a bit larger than the $\Delta\lambda_{abs}$ = +32 nm obtained with carboxylate–guanidinium pairs in **2a** (Figure 4). This result indicated that antiparallel ion pair–π interactions exist also without support from π–π interactions and hydrogen bonding, and confirmed that they are stronger in the more polarized excited state ES_a-**A** than in the less polarized ground state (Figure 5).

Unlike **2a**, the absorption maximum of **3a** was not fully solvent independent (Figure 3a vs b). A weakly negative solvatochromism brought the maxima in polar solvents closer to the maximal λ_{abs} = 430 nm of control **2o** without ion pair–π interactions (Figure 3a vs c, left, blue to red; Table 1, entries 13–18). With ion pairs lacking support from hydrogen bonding

DOI: 10.1021/jacs.5b05593
J. Am. Chem. Soc. 2015, 137, 11047–11056

and $\pi-\pi$ interactions, stronger contributions from the open **2a**–**o** and **ES$_a$-B** in more polar solvents could account for this trend (Figure 5). The same trends were found in the emission spectra (Figure 3a, right; Table 1, entries 13–18).

Titrations with TFA were performed in THF to avoid eventual solubility problems. The absorption spectra of **3a** were insensitive to TFA (Figure 7a, × symbols, and c). In clear contrast, the absorption maxima of **2a** shifted to the blue in response to the addition of TFA (Figure 7a, + symbols, and b). This acid sensitivity of **2a** was consistent with the destruction of the red-shifting antiparallel ion pair–π interaction by protonation of the carboxylate, i.e., formation of the open cation **2a**$^+$ (Figure 7). The acid insensitivity of the antiparallel ion pair in **3a** was in agreement with the poor basicity of the sulfonate anion.

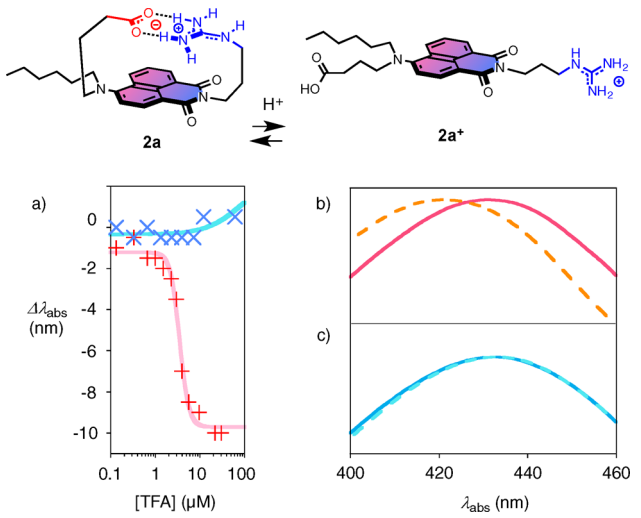

Figure 7. Changes in the absorption spectra of **2a** (2.0 μM, +) and **3a** (2.0 μM, ×) in THF with increasing concentrations of TFA (a), with examples for **2a** (b) and **3a** (c) without (solid) and with TFA (dashed), and indication of the structural basis of the sensitivity found with **2a**.

Time-Resolved Fluorescence. Time-resolved fluorescence measurements were performed using the time-correlated single-photon counting technique.[17] For parallel ion pair–π system **1p** and the open control **1o** in CCl_4, fluorescence decay after excitation with a laser pulse of 60 ps at 395 nm was monoexponential (Figure 8b). The lifetime of their excited states was nearly identical (Table 2, entries 4 and 5). This insensitivity of fluorescent lifetimes to parallel ion pair–π interactions was consistent with their removal by intramolecular proton transfer in the excited state.

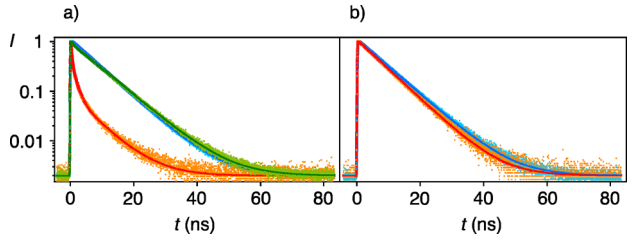

Figure 8. Time-resolved fluorescence decay of **1a** (a), **1p** (b), and **1o** (blue) in CCl_4 under neutral (red) and acidic conditions (green). Results from data analysis are listed in Table 2 (entries 1, 3–5).

Fluorescence decay kinetics of the antiparallel ion pair–π system **1a** in neutral CCl_4 were biphasic (Figure 8a, red). The main component of 87% had a lifetime of 0.98 ns, the residual 13% a lifetime of 6.5 ns (Table 2, entry 1). The short-lived excited state of **1a** around 1 ns fully disappeared with the removal of the antiparallel ion pair–π interactions by protonation of the carboxylate (Table 2, entry 3; compare Figure 7). However, it did not disappear with dilution. On the contrary, a new component with an ultrashort lifetime of 190 ps appeared at higher concentrations of **1a** (Table 2, entry 2). These trends suggested that the concentration independent fast component of **1a** around 1 ns originates from **ES$_a$-A** with intact and strong antiparallel ion pair–π interactions to stabilize the polarized excited state, whereas the minority component around 7 ns originates from the unfavorable but more emissive open **ES$_a$-B** without ion pair–π interactions (Figure 5). The presence of minor populations of **ES$_a$-B** was consistent with the dependence of the emission maxima on solvent polarity of **2a** and **3a** in steady-state measurements (Table 1).

With evidence against aggregation as origin of the 1 ns component of **1a** and **2a** in hand (Table 2, entries 1, 2, 6, and 9), deuterium exchange experiments were considered next. However, unchanged biexponential decay of **2a** in THF with 2% D_2O excluded proton transfer processes as well (Table 2, entries 9 and 10). Excited-state stabilization by antiparallel ion pair–π interactions as such seemed insufficient to account for the difference in lifetime between **1a**/**2a** and **1o**/**2o**. The mechanistic origin of the short lifetime of **ES$_a$-A** with strong antiparallel ion pair–π interactions thus remains to be unraveled, photoinduced electron transfer from pair to plane or in the other direction will be explored next (Figure 5).

Excited-State Geometry Optimization. Computational models of **1a** and **1p** in the ground state provided theoretical confirmation that ion pair–π interactions are energetically favorable.[13] The distances between the co-planar ions and π surface were taken as an indication for the strength of the interactions. In the ground state, parallel ion pair–π interactions in **1p** were identified as favorable despite repulsion from the push–pull dipole (Table 3, entry 2; Figure 9, bottom left, red structure). So far, proton transfer from guanidinium to carboxylate to neutralize the ion pair and thus remove dipole repulsion was not observed in the ground state (Figure 9, bottom left, red circle). Longer distances d_G were found for both ions with antiparallel ion pair–π interactions in **1a** in the ground state (Table 3, entry 1; Figure 9, top left, red structure).

The ground-state geometries of ref 13 were used as a starting point to minimize the structures of the excited states. Much too demanding for inclusion in the preliminary communication on the topic,[13] excited-state geometries were calculated with the second-order approximate coupled cluster method (CC2),[18] as implemented in TURBOMOLE v6.5.[19] For **1a**, the distances between both ions and the aromatic surface decreased clearly in the excited state (Figure 9, top left, blue structure; Table 3, entry 1). The attraction of the ion pair to the polarized surface of the excited fluorophore was consistent with strengthened antiparallel ion pair–π interactions in the excited state. This result was important because it provided theoretical support that the red shifts observed consistently with **1a**-**3a** originate indeed from **ES$_a$-A**, i.e., ion pair–π attraction in the excited state (Figure 5). The computed red shift in vacuum was remarkably close to the shifts measured in CCl_4 (Table 3, entries 1 and 3).

DOI: 10.1021/jacs.5b05593
J. Am. Chem. Soc. 2015, 137, 11047–11056

Table 2. Time-Resolved Fluorescence of Parallel and Antiparallel Ion Pair−π Interactions[a]

entry	solvent	cpd[b]	τ_1[c] (ns)	α_1[d] (%)	τ_2[c] (ns)	α_2[d] (%)	τ_3[c] (ns)	α_3[d] (%)	$\langle\tau\rangle$[e] (ns)
1	CCl_4 (neutral)	**1a**[f]			0.98	87	6.5	13	1.7
2	CCl_4 (neutral)	**1a**[g]	0.19	72	1.2	23	6.8	5	0.75
3	CCl_4 (acidic)	**1a**					7.2	100	7.2
4	CCl_4 (neutral)	**1p**					7.8	100	7.8
5	CCl_4 (neutral)	**1o**					7.6	100	7.6
6	toluene	**2a**			1.1	23	7.2	77	5.8
7		**2p**					8.6	100	8.6
8		**2o**					7.6	100	7.6
9	THF (2% H_2O)	**2a**			1.6	65	6.8	35	3.5
10	THF (2% D_2O)	**2a**			1.5	68	7.2	32	3.3

[a]Excitation was performed with a 60 ps laser pulse at 395 nm; sample concentrations were kept constant. [b]For structures, see Figures 1 and 2. [c]Time constants τ_i obtained from fluorescence time profiles (e.g., Figure 8). [d]Relative amplitude α_i of the component characterized by τ_i. [e]Average time constant $\langle\tau\rangle = \sum\alpha_i\tau_i$. [f]Measured at 6 μM. [g]Measured at 21 μM.

Table 3. Computational Data for Parallel and Antiparallel Ion Pair−π Interactions[a]

		anion−π[c]			cation−π[d]				
entry	cpd[b]	d_G (Å)	d_E (Å)	$d_E - d_G$ (Å)	d_G (Å)	d_E (Å)	$d_E - d_G$ (Å)	λ_{abs}[e] (nm)	E_{abs}[f] (eV)
1	**1a**	3.306	3.066	−0.240	3.305	3.136	−0.169	433	2.8660
2	**1p**	3.124	3.030	−0.094	2.905	3.135	+0.237	374	3.3163
3	**1o**							370	3.3483

[a]Calculated with TURBOMOLE v6.5, CC2. [b]For structures, see Figure 1. [c]Distances between anion and aromatic planes in ground state (d_G) and excited state (d_E), and the difference between the two ($d_E - d_G$). [d]Same as footnote *c*, but for the distances between cation and aromatic plane. [e]Calculated absorption maximum. [f]Calculated absorption energy.

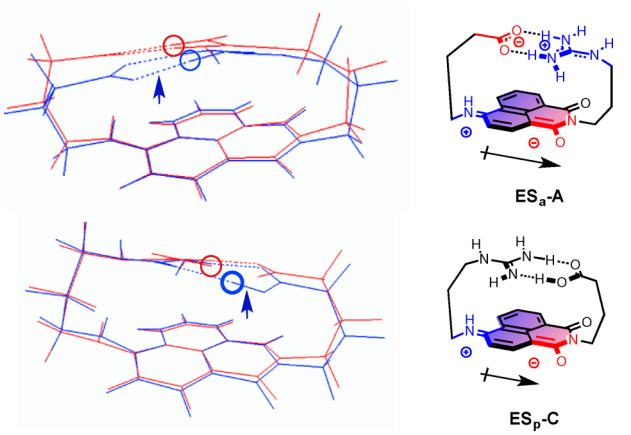

Figure 9. Energy-minimized structures of **1a** (top) and **1p** (bottom) in the ground state (red) and the excited state (blue). Arrows and circles indicate the absence of proton transfer in **ES$_a$-A** with antiparallel ion pair−π attraction in the ground and excited states (top) and the presence of proton transfer not in the ground state (bottom, red circle) but in **ES$_p$-C** in response to parallel ion pair−π repulsion in the excited state (bottom, blue circle, blue arrow).

In the parallel **1p**, the complementary parallel ion pair−π repulsion in the excited state was not clearly visible (Figure 9, bottom left, blue structure; Table 3, entry 2). This absence of consistently increased distances between the parallel ion pair and polarized surface in the excited state was understandable because the ion pair is neutralized by proton transfer from the guanidinium cation to the carboxylate anion (Figure 9, bottom left, blue structure, arrow). A neutral excited state **ES$_p$-C** without parallel ion pair−π repulsion was in excellent agreement with the similarity of the emission spectra of **2p** and ion-pair-free control **1o** (Figures 3 and 8). The absence of proton transfer in the computed ground-state structure of **1p** was in agreement with the strong shifts in the NMR spectra of **1** and **2** (Figure 9, bottom left, red circle; Figures 1 and 2). It was also meaningful because the ground state is less polarized, parallel ion pair−dipole repulsion thus weaker, and deprotonation of the poorly acidic guanidinium cation generally very unfavorable.[8]

Semi-covalent Systems. These coherent and supportive results for the existence and significance of ion pair−π interactions in covalent systems called for binding studies. Following previous reports,[6] the influence of a polarized π surface on ion binding was evaluated by monitoring the exchange of weaker counterions by stronger ones. For cation binding by antiparallel and parallel ion pair−π interactions, the guanidinium cations in **2a** and **2p** were removed and replaced by solubilizing alkyl chains. For the complementary anion binding by antiparallel and parallel ion pair−π interactions, the carboxylate anions in **2a** and **2p** were replaced by the same alkyl chains. The anionic and cationic ANIs **4** and **5** were easily accessible, following the synthetic methods outlined above for the covalent systems (Figure 10 and Schemes 1, 2, S2, and S3).

Anion-exchange studies were performed by ^{1}H NMR spectroscopy. The titration of the chloride salts of **5a** and **5p** with the triethylammonium salt of carboxylate **5c** in perdeuterated THF is shown as a representative example (Figure 11). With increasing carboxylate concentrations, the chemical shifts of the naphthalene protons and the protons in the Leonard turns changed. These changes differed from proton to proton. For anion binding by antiparallel ion pair−π interactions, the shifts in the naphthalene region of **5a** were most impressive (Figure 11a). In the downfield region of the spectra, strongest shifts occurred with the proton attached to carbons 5 and 6, followed by proton 7, whereas the protons 3 and particularly 2 were much less responsive to anion exchange. This selective sensitivity was in support of intermolecular anion−π interactions that take place on the surface of the

DOI: 10.1021/jacs.5b05593
J. Am. Chem. Soc. 2015, 137, 11047−11056

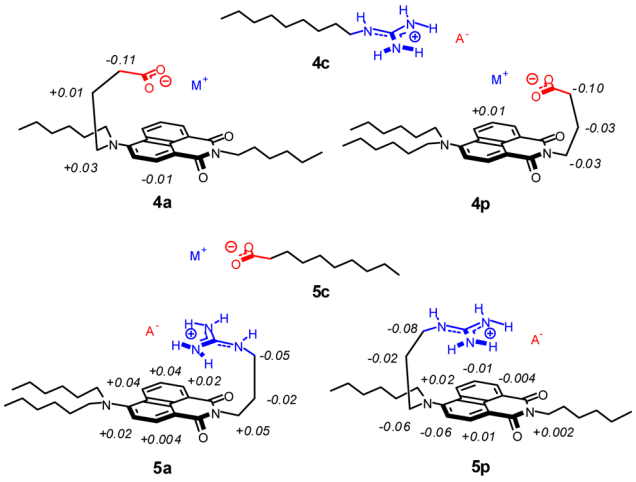

Figure 10. Semi-covalent systems **4a** and **4p** (M^+ = triethylammonium) for antiparallel and parallel binding of counterion **4c** (A^- = PF_6^-) and **5a** and **5p** (A^- = Cl^-) for antiparallel and parallel binding of counterion **5c** (M^+ = triethylammonium) by ion pair–π interactions. Shifts in the ^{1}H NMR spectral signals in response to ion exchange are indicated in ppm (compare Figure 11).

naphthalene, and suggested that they might occur preferably on the aromatic ring without amine donor.

For anion binding by parallel ion pair–π interactions in **5p**, the shifts in the naphthalene region were overall smaller (Figure 11c). This reduced sensitivity of the naphthalene region to anion exchange was meaningful because for parallel ion pair–π interactions in **5p**, the intermolecular anion–π interactions should occur on the NMR-silent pyridinedione heterocycle. The strongest shifts were found with proton 3, possibly because the guanidinium cation resides more on this side of the naphthalene. Interestingly, this most upfield shifted proton 3 was less sensitive to the antiparallel ion pair–π interactions in **5a** (Figure 11a).

In the Leonard turns to the guanidinium cations, it was important that anion binding by both **5a** and **5p** caused larger shifts for protons 1′ and 3′ than for 2′ (Figure 11a,c). This strong response at both ends but not in the middle of the turns supported that the aromatic system participates in the ion pairing between carboxylate and guanidinium, i.e., the occurrence of ion pair–π interactions. These shifts in turn and plane were of general importance because the direct observation of anion–π interactions by ^{1}H NMR spectroscopy in similarly pure systems without assistance from other interactions in more refined binding sites, and thus with overall very weak affinity, has been notoriously difficult.[20]

Cation binding for **4a** and **4p** was followed in the same way but was overall less interesting because cation–π interactions[5] are much better established than anion–π interactions.[1−4] Whereas NMR shifts in the turns were as strong as with anion binding to **5**, NMR shifts in the plane of **4** were weaker (Figure 10). As with anion binding, shifts at both ends equal or exceeding those in the middle of the Leonard turns supported that the aromatic system participates in the binding of cations as well.

Illustrating nicely the advantage of covalent approaches to explore ion pair–π interactions as described above, the dependence of the NMR shifts on the concentration of the added ions was in part quite complex. It often differed from proton to proton and could show indications for possible contributions from higher-order binding modes (Figure 11).

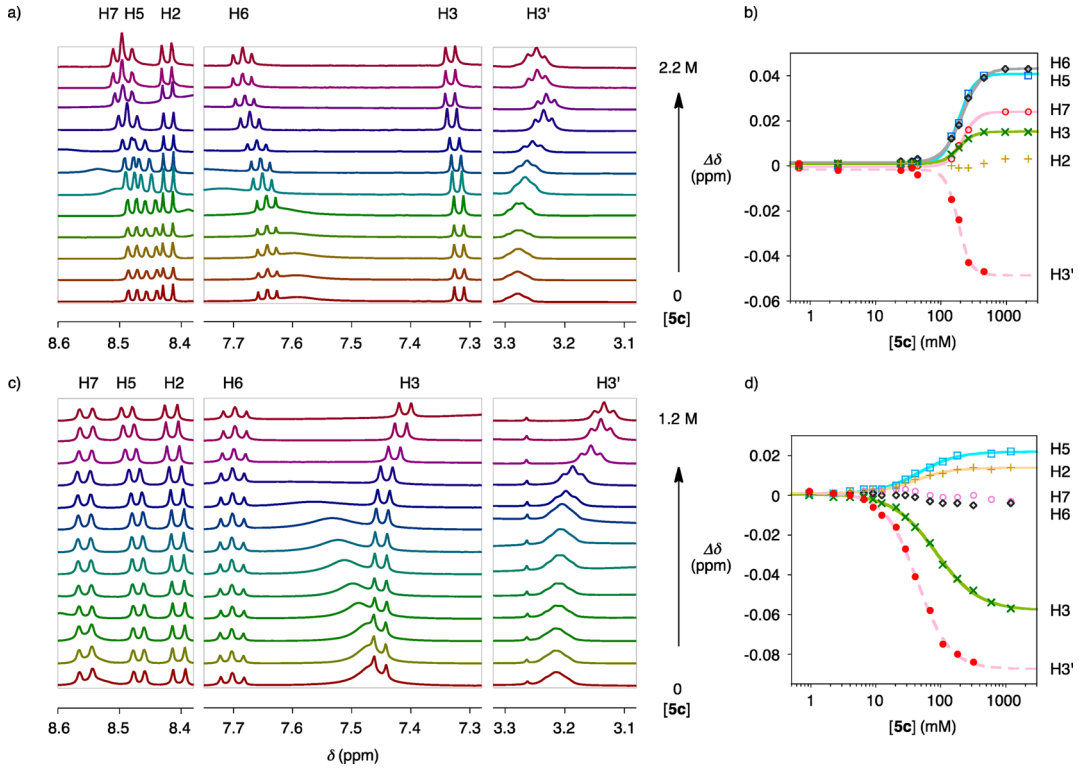

Figure 11. ^{1}H NMR spectra of **5a** (11 mM, a) and **5p** (11 mM, c) in perdeuterated THF in the presence of increasing concentrations of **5c**, and dose–response curves for the most responsive protons in **5a** (b) and **5p** (d) (compare Figure 10 for structures and Schemes 1 or 2 for carbon numbering).

DOI: 10.1021/jacs.5b05593
J. Am. Chem. Soc. 2015, 137, 11047−11056

This quite complex behavior was not surprising considering that coupled ion-exchange processes are observed in the millimolar range, with very small differences between necessarily very weak binders rather than fully developed receptors. Further interpretation including quantitative analysis was thus not appropriate[21] except for the observation that anion exchange with parallel ion pair–π interactions occurred at clearly lower concentrations than anion exchange with antiparallel ion pair–π interactions (Figures 11b,d; anion exchange with **4c** was in the range of antiparallel **5a**). This was consistent with predictions from theory that, in contrast to the preference for antiparallel ion pair–π interactions in the excited state, parallel ion pair–π interactions should be preferred on push–pull surfaces in the ground state, despite repulsion form push–pull dipoles (Table 3). Not obvious for cation binding in solution (Figure S2), the same preference for parallel ion pair–π interactions was also observed for cations in the context of cell-penetrating peptides.

Activation of Cell-Penetrating Peptides. Earlier, we have speculated that ion pair–π interactions could account for the exceptional ability of pyrenebutyrate to activate arginine-rich CPPs[8,22,23] and their mimics.[24] These intriguing polycations can cross lipid bilayer membranes of model vesicles as well as cells via transient binding to hydrophobic anions present in the membrane.[8,22−25] Although cell membranes contain intrinsic anionic lipids, the activity of CPPs could be further enhanced by extrinsic amphiphilic anions.[8] For the best CPP activator, i.e., pyrenebutyrate,[8,22] computational studies indicated that the formation of guanidinium–carboxylate pairs on π-basic surface of pyrene is energetically favorable.[13] The question whether or not oriented ion pair–π interactions on the push–pull surfaces of the anionic amphiphiles **4a** and **4p** could influence CPP activation was thus most intriguing.

CPP activators are routinely characterized with the CF assay.[8,23] In this assay, large unilamellar vesicles (LUVs) composed of egg yolk phosphatidylcholine (EYPC) are loaded with 5(6)-carboxyfluorescein (CF) at concentrations high enough for self-quenching to occur. CF export is then recorded as fluorescence recovery because self-quenching decreases upon local CF dilution. Poly-L-arginine is used here as standard CPP to evaluate counterion activators.[8,21] Without activators, poly-L-arginine is inactive in EYPC-LUVs⊃CF. Addition of 2 μM pyrenebutyrate 50 s after the beginning of a measurement did not cause CF release (Figure 12a, dotted, gray). At this low concentration, pyrenebutyrate also failed to activate poly-L-arginine added 50 s later (Figure 12b, dotted, gray).

In the same CF assay, the addition of 2 μM **4a** and **4p** also did not cause CF release (Figure 12a, solid and dashed). This inactivity without poly-L-arginine demonstrated that neither of the amphiphiles acts as detergents at low enough concentrations. Upon addition of poly-L-arginine to LUVs loaded with 2 μM **4a** and **4p**, significant CF release was observed. The ability of **4p** (Figure 12b, solid, red) to activate poly-L-arginine as anion transporter exceeded that of **4a** clearly (Figure 12b, dashed, blue).

For several reasons, including proximity effects from intramolecular charge repulsion,[8,22−25] EC_{50}'s measured for guanidinium-rich polymers in vesicles (Figure 12) are always much below the millimolar range characteristic for monomeric ion pairing in solution (Figures 11 and S2). Dose–response curves confirmed that **4a** and **4p** were much more active than pyrenebutyrate, characterized by EC_{50} = 19.5 ± 1.0 μM under the present conditions. Dose–response curves further confirmed that **4p** (EC_{50} = 1.05 ± 0.05 μM) is more active than **4a** (EC_{50} = 3.6 ± 0.2 μM). The difference in CPP activation corresponded very well with the preferred formation of parallel ion pair–π interactions in **5p** compared to antiparallel ion pair–π interactions in **5a** (Figure 11) and computational results for **1p** and **1a** (Table 3). Considering the many parameters contributing to activity in lipid bilayer membranes, this finding does by no means demonstrate that ion pair–π interactions account for the activity of pyrenebutyrate, **4a**, and **4p** as activators of cell-penetrating peptides. However, the coincidence is interesting and deserves further attention.

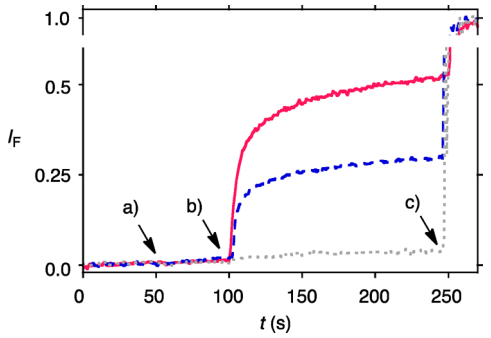

Figure 12. Fractional CF emission intensity I_F (λ_{ex} = 492 nm, λ_{em} = 517 nm) during the addition of pyrenebutyrate (gray, dotted), **4a** (blue, dashed), and **4p** (red, solid, 2 μM final concentration) after 50 s (a) and poly-L-arginine (0.25 μM) after 100 s (b) to EYPC-LUVs⊃CF (50 mM CF, 10 mM Na^+ phosphate, 10 mM NaCl, pH 7.4, 25 °C; calibrated by final addition of Triton X-100 (c)).

CONCLUSIONS

The objective of this study was to see whether anions and cations could interact with one and the same aromatic surface. This question was addressed first with a covalent approach to precisely position the ion pairs on the polarized surfaces of push–pull fluorophores, either in parallel or antiparallel orientation with respect to the push–pull dipole. With covalent systems in the ground state, the existence of parallel and antiparallel ion pair–π interactions was supported by shifts in the ^{1}H NMR spectra. Computational models indicate that parallel ion pair–π interactions are preferred.

Upon excitation, intramolecular charge transfer polarizes the surface of push–pull fluorophores. The stabilization of these polarized excited states by antiparallel ion pair–π attraction is demonstrated by red shifts of absorption and emission maxima. Computational models confirm that antiparallel ion pair–π interactions are stronger in the excited state than in the ground state. Time-resolved fluorescence measurements provide the essential quantitative experimental foundation for operational ion pair–π attraction on the polarized surfaces of excited push–pull fluorophores. The situation with parallel ion pair–π interactions in the excited state is more complex and involves charge neutralization by electron and proton transfer between the cation and the anion on the strongly polarized push–pull surface. Theoretical and experimental support for proton transfer from the poorly acidic guanidinium cations is also of biological interest because, in sharp contrast to the more acidic ammonium cation in lysines, the positive charge of arginine residues is commonly assumed to be permanent without exception and is proposed as the origin of much "arginine magic".[8,22−25]

DOI: 10.1021/jacs.5b05593
J. Am. Chem. Soc. 2015, 137, 11047−11056

To move beyond covalent systems, one of the two ions was removed. ^{1}H NMR ion-exchange studies with a complete set of semi-covalent systems support the presence of operational anion−π and cation−π interactions in parallel and antiparallel ion pair−π interactions in the ground state. Parallel ion pair−π interactions are identified as more powerful to bind anions. In agreement with computational data, this preference supports that on push−pull systems, anion−π interactions are best near the electron-withdrawing substituent and cation−π interactions near the donor, despite repulsion from the push−pull dipole.

The comprehensive and coherent results on ion pair−π interactions in covalent and semi-covalent systems reported in this study invite for future exploration. Attractive topics reach from the quite challenging theoretical basics to a broad range of appealing applications, reaching from catalysis[3−5] to cellular uptake.[22−25] Particularly the observation that ion pair−π interactions could possibly contribute to the activation of cell-penetrating peptides could deserve a closer look, also in live cells. For further development of ion pair−π interactions as such, the next challenge will concern completely non-covalent ion pair−π interactions, at best with one sodium cation and one chloride anion sitting next to each other on the surface of a push−pull chromophore.

■ ASSOCIATED CONTENT

Supporting Information

The Supporting Information is available free of charge on the ACS Publications website at DOI: 10.1021/jacs.5b05593.

Detailed experimental procedures (PDF)

■ AUTHOR INFORMATION

Corresponding Author

*stefan.matile@unige.ch

Notes

The authors declare no competing financial interest.

■ ACKNOWLEDGMENTS

We thank the NMR and the Sciences Mass Spectrometry (SMS) platforms for services, and the University of Geneva, the European Research Council (ERC Advanced Investigator), the National Centre of Competence in Research (NCCR) Molecular Systems Engineering, the NCCR Chemical Biology, and the Swiss NSF for financial support.

■ REFERENCES

(1) (a) Quinonero, D.; Garau, C.; Rotger, C.; Frontera, A.; Ballester, P.; Costa, A.; Deya, P. M. *Angew. Chem., Int. Ed.* **2002**, *41*, 3389−3392. (b) Mascal, M.; Armstrong, A.; Bartberger, M. D. *J. Am. Chem. Soc.* **2002**, *124*, 6274−6276. (c) Alkorta, I.; Rozas, I.; Elguero, J. *J. Am. Chem. Soc.* **2002**, *124*, 8593−8598. (d) Frontera, A.; Gamez, P.; Mascal, M.; Mooibroek, T. J.; Reedijk, J. *Angew. Chem., Int. Ed.* **2011**, *50*, 9564−9583. (e) Estarellas, C.; Frontera, A.; Quiñonero, D.; Deyà, P. M. *Angew. Chem., Int. Ed.* **2011**, *50*, 415−418. (f) Salonen, L. M.; Ellermann, M.; Diederich, F. *Angew. Chem., Int. Ed.* **2011**, *50*, 4808−4842. (g) Chifotides, H. T.; Dunbar, K. R. *Acc. Chem. Res.* **2013**, *46*, 894−906. (h) Ballester, P. *Acc. Chem. Res.* **2013**, *46*, 874−884. (i) Vargas Jentzsch, A.; Hennig, A.; Mareda, J.; Matile, S. *Acc. Chem. Res.* **2013**, *46*, 2791−2800. (j) Bauza, A.; Quinonero, D.; Deya, P. M.; Frontera, A. *Chem. - Eur. J.* **2014**, *20*, 6985−6990.

(2) (a) Rosokha, Y. S.; Lindeman, S. V.; Rosokha, S. V.; Kochi, J. K. *Angew. Chem., Int. Ed.* **2004**, *43*, 4650−4652. (b) Gorteau, V.; Bollot, G.; Mareda, J.; Perez-Velasco, A.; Matile, S. *J. Am. Chem. Soc.* **2006**, *128*, 14788−14789. (c) Maeda, H.; Morimoto, T.; Osuka, A.; Furuta, H. *Chem. - Asian J.* **2006**, *1*, 832−844. (d) Lakshminarayanan, P. S.; Ravikumar, I.; Suresh, E.; Ghosh, P. *Inorg. Chem.* **2007**, *46*, 4769−4771. (e) Wang, D.-X.; Zheng, Q. Y.; Wang, Q. Q.; Wang, M.-X. *Angew. Chem., Int. Ed.* **2008**, *47*, 7485−7488. (f) Chudzinski, M. G.; McClary, C. A.; Taylor, M. S. *J. Am. Chem. Soc.* **2011**, *133*, 10559−10567. (g) Wang, D.-X.; Wang, M.-X. *J. Am. Chem. Soc.* **2013**, *135*, 892−897. (h) Watt, M. M.; Zakharov, L. N.; Haley, M. M.; Johnson, D. W. *Angew. Chem., Int. Ed.* **2013**, *52*, 10275−10280. (i) Bretschneider, A.; Andrada, D. M.; Dechert, S.; Meyer, S.; Mata, R. A.; Meyer, F. *Chem. - Eur. J.* **2013**, *19*, 16988−17000. (j) Schneebeli, S. T.; Frasconi, M.; Liu, Z.; Wu, Y.; Gardner, D. M.; Strutt, N. L.; Cheng, C.; Carmieli, R.; Wasielewski, M. R.; Stoddart, J. F. *Angew. Chem., Int. Ed.* **2013**, *52*, 13100−13104. (k) Arranz-Mascroś, P.; Bazzicalupi, C.; Bianchi, A.; Giorgi, C.; Godino-Salido, M.-L.; Gutieŕrez-Valero, M.-D.; Lopez-Garzoń, R.; Savastano, M. *J. Am. Chem. Soc.* **2013**, *135*, 102−105. (l) Vargas Jentzsch, A.; Matile, S. *J. Am. Chem. Soc.* **2013**, *135*, 5302−5303. (m) Adriaenssens, L.; Estarellas, C.; Vargas Jentzsch, A.; Martinez Belmonte, M.; Matile, S.; Ballester, P. *J. Am. Chem. Soc.* **2013**, *135*, 8324−8330. (n) Zhao, Y.; Domoto, Y.; Orentas, E.; Beuchat, C.; Emery, D.; Mareda, J.; Sakai, N.; Matile, S. *Angew. Chem., Int. Ed.* **2013**, *52*, 9940−9943. (o) Adriaenssens, L.; Gil-Ramirez, G.; Frontera, A.; Quinonero, D.; Escudero-Adan, E. C.; Ballester, P. *J. Am. Chem. Soc.* **2014**, *136*, 3208−3218. (p) He, Q.; Han, Y.; Wang, Y.; Huang, Z.-T.; Wang, D.-X. *Chem. - Eur. J.* **2014**, *20*, 7486−7491. (q) Berkessel, A.; Das, S.; Pekel, D.; Neudörfl, J.-M. *Angew. Chem., Int. Ed.* **2014**, *53*, 11660−11664. (r) Giese, M.; Albrecht, M.; Valkonen, A.; Rissanen, K. *Chem. Sci.* **2015**, *6*, 354−359. (s) Hafezi, N.; Holcroft, J. M.; Hartlieb, K. J.; Dale, E. J.; Vermeulen, N. A.; Stern, C. L.; Sarjeant, A. A.; Stoddart, F. J. *Angew. Chem.* **2015**, *127*, 466−471.

(3) Zhao, Y.; Beuchat, C.; Mareda, J.; Domoto, Y.; Gajewy, J.; Wilson, A.; Sakai, N.; Matile, S. *J. Am. Chem. Soc.* **2014**, *136*, 2101−2111.

(4) Zhao, Y.; Sakai, N.; Matile, S. *Nat. Commun.* **2014**, *5*, 3911.

(5) (a) Dougherty, D. A. *Acc. Chem. Res.* **2013**, *46*, 885−893. (b) Mahadevi, A. S.; Sastry, G. N. *Chem. Rev.* **2013**, *113*, 2100−2138. (c) Yamada, S.; Fossey, J. S. *Org. Biomol. Chem.* **2011**, *9*, 7275−7281. (d) Holland, M. C.; Metternich, J. B.; Mück-Lichtenfeld, C.; Gilmour, R. *Chem. Commun.* **2015**, *51*, 5322−5325.

(6) (a) Rensing, S.; Arendt, M.; Springer, A.; Grawe, T.; Schrader, T. *J. Org. Chem.* **2001**, *66*, 5814−5821. (b) Thompson, S. E.; Smithrud, D. B. *J. Am. Chem. Soc.* **2002**, *124*, 442−449. (c) Haj-Zaroubi, M.; Schmidtchen, F. P. *ChemPhysChem* **2005**, *6*, 1181−1186. (d) Blondeau, P.; Segura, M.; Perez-Fernandez, R.; de Mendoza, J. *Chem. Soc. Rev.* **2007**, *36*, 198−210. (e) Wang, X.; Post, J.; Hore, D. K.; Hof, F. *J. Org. Chem.* **2014**, *79*, 34−40. (f) Perraud, O.; Robert, V.; Gornitzka, H.; Martinez, A.; Dutasta, J.-P. *Angew. Chem., Int. Ed.* **2012**, *51*, 504−508. (g) Wang, X.; Sarycheva, O. V.; Koivisto, B. D.; McKie, A. H.; Hof, F. *Org. Lett.* **2008**, *10*, 297−300. (h) Jenkins, D. D.; Harris, J. B.; Howell, E. E.; Hinde, R.; Baudry, J. *J. Comput. Chem.* **2013**, *34*, 518−522.

(7) (a) Feliciano, G. T.; da Silva, A. J. R.; Reguera, G.; Artacho, E. *J. Phys. Chem. A* **2012**, *116*, 8023−8030. (b) Gao, J.; Müller, P.; Wang, M.; Eckhardt, S.; Lauz, M.; Fromm, K. M.; Giese, B. *Angew. Chem., Int. Ed.* **2011**, *50*, 1926−1930. (c) Barnett, R. N.; Cleveland, C. L.; Joy, A.; Landman, U.; Schuster, G. B. *Science* **2001**, *294*, 567−571. (d) Yasutomi, S.; Morita, T.; Kimura, S. *J. Am. Chem. Soc.* **2005**, *127*, 14564−14565. (e) Sakai, N.; Charbonnaz, P.; Ward, S.; Matile, S. *J. Am. Chem. Soc.* **2014**, *136*, 5575−5578.

(8) Sakai, N.; Matile, S. *J. Am. Chem. Soc.* **2003**, *125*, 14348−14356.

(9) Sheves, M.; Nakanishi, K.; Honig, B. *J. Am. Chem. Soc.* **1979**, *101*, 7086−7088.

(10) (a) Kiser, P. D.; Golczak, M.; Palczewski, K. *Chem. Rev.* **2014**, *114*, 194−232. (b) Zhou, X.; Sundholm, D.; Wesolowski, T. A.; Kaila, V. R. I. *J. Am. Chem. Soc.* **2014**, *136*, 2723−2726. (c) Nielsen, M. B. *Chem. Soc. Rev.* **2009**, *38*, 913−924.

(11) (a) Ai, H. W.; Olenych, S. G.; Wong, P.; Davidson, M. W.; Campbell, R. E. *BMC Biol.* **2008**, *6*, 13. (b) List, N. H.; Olsen, J. M. H.; Jensen, H. J. A.; Steindal, A. H.; Kongsted, J. *J. Phys. Chem. Lett.* **2012**, *3*, 3513−3521. (c) Cai, D.; Marques, M. A. L.; Nogueira, F. *J. Phys. Chem. B* **2013**, *117*, 13725−13730.

DOI: 10.1021/jacs.5b05593
J. Am. Chem. Soc. 2015, 137, 11047−11056

(12) Mitra, M.; Manna, P.; Seth, S. K.; Das, A.; Meredith, J.; Helliwell, M.; Bauzá, A.; Choudhury, S. R.; Frontera, A.; Mukhopadhyay, S. *CrystEngComm* **2013**, *15*, 686−696.
(13) Fujisawa, K.; Beuchat, C.; Humbert-Droz, M.; Wilson, A.; Wesolowski, T. A.; Mareda, J.; Sakai, N.; Matile, S. *Angew. Chem., Int. Ed.* **2014**, *53*, 11266−11269.
(14) (a) Reichardt, C. *Chem. Rev.* **1994**, *94*, 2319−2358. (b) Reichart, C.; Welton, T. *Solvents and Solvent Effects in Organic Chemistry*, 4th ed.; Wiley-VCH: Weinheim, 2011; pp 359−424. (c) Suppan, P.; Ghoneim, N. *Solvatochromism*; The Royal Society of Chemistry: Cambridge, 1997, 1−259. (d) Liess, A.; Huang, L.; Arjona-Esteban, A.; Lv, A.; Gsänger, M.; Stepanenko, V.; Stolte, M.; Würthner, F. *Adv. Funct. Mater.* **2015**, *25*, 44−57. (e) Lindquist, R. J.; Lefler, K. M.; Brown, K. E.; Dyar, S. M.; Margulies, E. A.; Young, R. M.; Wasielewski, M. R. *J. Am. Chem. Soc.* **2014**, *136*, 14912−14923. (f) Miller, W.; Lin, J. Y.; Frady, E. P.; Steinbach, P. A.; Kristan, W. B., Jr; Tsien, R. Y. *Proc. Natl. Acad. Sci. U. S. A.* **2012**, *109*, 2114−2119.
(15) (a) Duke, R. M.; Veale, E. B.; Pfeffer, F. M.; Kruger, P. E.; Gunnlaugsson, T. *Chem. Soc. Rev.* **2010**, *39*, 3936−3953. (b) de Silva, A. P.; Gunaratne, H. Q. N.; Habib-Jiwan, J.-L.; McCoy, C. P.; Rice, T. E.; Soumillion, J.-P. *Angew. Chem., Int. Ed. Engl.* **1995**, *34*, 1728−1731. (c) Greenfield, S. R.; Svec, W. A.; Gosztola, D.; Wasielewski, M. R. *J. Am. Chem. Soc.* **1996**, *118*, 6767−6777.
(16) (a) Browne, D. T.; Eisinger, J.; Leonard, N. J. *J. Am. Chem. Soc.* **1968**, *90*, 7302−7323. (b) Leonard, N. J. *Acc. Chem. Res.* **1979**, *12*, 423−429.
(17) Muller, P. A.; Hogemann, C.; Allonas, X.; Jacques, P.; Vauthey, E. *Chem. Phys. Lett.* **2000**, *326*, 321−327.
(18) Köhn, A.; Hättig, C. *J. Chem. Phys.* **2003**, *119*, 5021−5036.
(19) *TURBOMOLE* v6.5, 2013, a development of University of Karlsruhe and Forschungszentrum Karlsruhe GmbH, 1989−2007, TURBOMOLE GmbH, since 2007; available from http://www.turbomole.com.
(20) Dawson, R. E.; Hennig, A.; Weimann, D. P.; Emery, D.; Ravikumar, V.; Montenegro, J.; Takeuchi, T.; Gabutti, S.; Mayor, M.; Mareda, J.; Schalley, C. A.; Matile, S. *Nat. Chem.* **2010**, *2*, 533−538.
(21) (a) Bindslev, N. *Drug-Acceptor Interactions. Modeling Theoretical Tools to Test and Evaluate Experimental Equilibrium Effects*; Co-Action Publishing: Järfälla, Sweden, 2008; pp 257−282. (b) Shoichet, B. K. *J. Med. Chem.* **2006**, *49*, 7274−7277. (c) Bhosale, S.; Matile, S. *Chirality* **2006**, *18*, 849−856.
(22) (a) Takeuchi, T.; Kosuge, M.; Tadokoro, A.; Sugiura, Y.; Nishi, M.; Kawata, M.; Sakai, N.; Matile, S.; Futaki, S. *ACS Chem. Biol.* **2006**, *1*, 299−303. (b) Katayama, S.; Nakase, I.; Yano, Y.; Murayama, T.; Nakata, Y.; Matsuzaki, K.; Futaki, S. *Biochim. Biophys. Acta, Biomembr.* **2013**, *1828*, 2134−2142.
(23) Perret, F.; Nishihara, M.; Takeuchi, T.; Futaki, S.; Lazar, A. N.; Coleman, A. W.; Sakai, N.; Matile, S. *J. Am. Chem. Soc.* **2005**, *127*, 1114−1115.
(24) Hennig, A.; Gabriel, G. J.; Tew, G. N.; Matile, S. *J. Am. Chem. Soc.* **2008**, *130*, 10338−10344.
(25) (a) Sakai, N.; Futaki, S.; Matile, S. *Soft Matter* **2006**, *2*, 636−641. (b) Stanzl, E. G.; Trantow, B. M.; Vargas, J. R.; Wender, P. A. *Acc. Chem. Res.* **2013**, *46*, 2944−2954. (c) Bechara, C.; Sagan, S. *FEBS Lett.* **2013**, *587*, 1693−1702. (d) Whitney, M.; Savariar, E. N.; Friedman, B.; Levin, R. A.; Crisp, J. L.; Glasgow, H. L.; Lefkowitz, R.; Adams, S. R.; Steinbach, P.; Nashi, N.; Nguyen, Q. T.; Tsien, R. Y. *Angew. Chem., Int. Ed.* **2013**, *52*, 325−330. (e) Schmidt, D.; Jiang, Q. X.; MacKinnon, R. *Nature* **2006**, *444*, 775−779.

DOI: 10.1021/jacs.5b05593
J. Am. Chem. Soc. 2015, 137, 11047−11056